



Nanoparticle sizing with a resolution beyond the diffraction limit using UV light scattering spectroscopy

Kun Chen ^{a,*}, Alexey Kromin ^a, Melville P. Ulmer ^b, Bruce W. Wessels ^c,
Vadim Backman ^{a,*,1}

^a Department of Biomedical Engineering, Northwestern University, Evanston, IL 60208, USA

^b Department of Physics and Astronomy, Northwestern University, Evanston, IL 60208, USA

^c Department of Materials Science and Engineering, Northwestern University, Evanston, IL 60208, USA

Received 9 August 2003; received in revised form 19 September 2003; accepted 23 September 2003

Abstract

We investigated the detection of dielectric nanoparticles using static light scattering spectroscopy (LSS) in the UV range (from 250 to 390 nm). The light scattered by the polystyrene nanospheres in the backward direction were collected by means of an optical fiber probe and a charge-coupled device (CCD) spectrograph. The size distributions of the nanoparticles were obtained by a discrete inverse on the backscattering spectra using a theoretical model based on Mie theory. Our results show that UV LSS can be used to measure the sizes of nanoparticles with an accuracy far exceeding the diffraction limit and to study subwavelength structures at nanometer scale. This technique may find potential scientific and industrial applications including the study of macromolecular complexes at nanoscale, detection and identification of viral particles, non-invasive probing of nanoscale surface structures, and monitoring the processing of pharmaceutical nanoparticles.

© 2003 Elsevier B.V. All rights reserved.

PACS: 87.64.Cc

Keywords: Nanosphere; Biomedical optics; Mie theory; Light scattering spectroscopy

1. Introduction

Nanoparticle size analysis has profound importance in many fields. For example, semicon-

ductor nanocrystals exhibit size dependent optical and electronic properties [1,2]. Viruses are nanometer scale particles consisting of proteins and genetic materials, and virus sizes play an important role in their resistance to disinfectant chemical agents [3]. Cellular macromolecular complexes, which govern most cell functions, are typically within the range of a few tens of nanometers. Therefore, accurate determination of the sizes of these nanoscale objects will improve our

* Corresponding authors. Tel.: +1-847-491-7167; fax: +1-847-491-4928.

E-mail addresses: k-chen7@northwestern.edu (K. Chen), v-backman@northwestern.edu (V. Backman).

¹ Tel.: +1-847-491-3536; fax: +1-847-491-4928.

understanding of their functioning and behavior. To achieve this, a non-invasive and real-time imaging technique with superresolution at nanometer scales is necessary. However, current techniques capable of nanoscale resolution have multiple limitations. Electron microscopy [4,5] requires the sample to be fixed and stained with contrast agents, which inevitably introduces artifacts and in the meantime forbids *in vivo* detections. Near-field scanning optical microscopy (NSOM) [6–8] and atomic force microscopy (AFM) [9–12] are both scanning techniques and require long data acquisition times. In addition, their short-range imaging capability forbids their applications from imaging cell interiors.

Optical techniques not only have the advantage of non-invasiveness, but also carry chemical information about samples. Traditionally, optical microscopy has been applied to study microstructures. However, it cannot avoid a fundamental limit in its achievable spatial resolution, which is dictated by the diffraction of light and equals approximately to half of the wavelength of the light used. In the visible range, the theoretically achievable resolution is ~ 300 nm. Another well-established technique, dynamic light scattering (DLS), requires the scattering particles to have substantial diffusion rate, in order to achieve high accuracy. This condition is not satisfied in many cases. For example, the quantum dots are localized in the process of semiconductor crystal growth. Moreover, in most cellular environments, subcellular contents do not follow diffuse motion.

In recent years there have been active developments in particle sizing using various optical approaches. Alexander and Hallett [13] collected small-angle light scattering from monodispersed polystyrene spheres at the wavelength 632.8 nm. They then successfully extracted the size distribution of the spheres by analyzing the angular distribution of the scattered light in the forward cone. However, this technique is not suited for the direct determination of particle diameters smaller than 300 nm [13], and essentially has not broken the diffraction limit. In another development, light scattering spectroscopy (LSS) in the visible range has been applied to predict the size distributions of scattering polystyrene spheres [14] and cell nuclei

[15,16], for the purpose of early diagnosis of human epithelial precancers. It has been discovered that the shapes of light scattering spectra are distinguishable for particles that are much larger than the wavelength of light λ but differ in size by as small as $\lambda/10$, and the particle size information can be obtained by analyzing these spectral shapes.

In this paper, we report experimental and theoretical work on identifying nanosphere sizes using LSS in the UV range ($\lambda \sim 250\text{--}390$ nm). A resolution within 10 nm has been achieved, far exceeding the diffraction limit. Compared with LSS in the visible range, UV light scattering may have additional advantages specifically for biomedical applications, as DNA and proteins exhibit characteristic absorption features in the UV range. The carcinogenic nature of UV radiation should not be a concern when UV LSS analysis is performed on excised tissue specimens or cell cultures. Further, biological applications on relatively simple structures, such as detecting viral particles and studying macromolecular complexes, and non-biological applications, including non-invasive probing of nanoscale surfaces structures, can be explored.

2. Experiment

The experiments were conducted on monodispersed suspensions of polystyrene nanospheres (Duke Scientific, Inc.). Four samples were prepared by diluting water solutions of single-sized spheres to 0.01 wt.% concentration (i.e., 9.5×10^{-5} volume fraction). Their mean sizes and standard deviations were 33 ± 3.6 , 41 (standard deviation unspecified), 63 ± 9.5 and 81 ± 5.8 nm, respectively. Each solution was then transferred onto a glass slide to create an optically thin monolayer of scatterers. An optical fiber probe (Fig. 1) was designed to deliver light to the sample and collect the scattered light in the backward direction. The probe consisted of five silica multimode fibers (Thorlabs, Inc.), each with 200- μm core diameter and 0.22 numerical aperture. The central fiber served as the delivery channel, while the four collection fibers were arranged on a ring of 0.75-mm radius. In the experimental setup (Fig. 1), a 75W Xenon lamp (Oriel Instruments) provided the

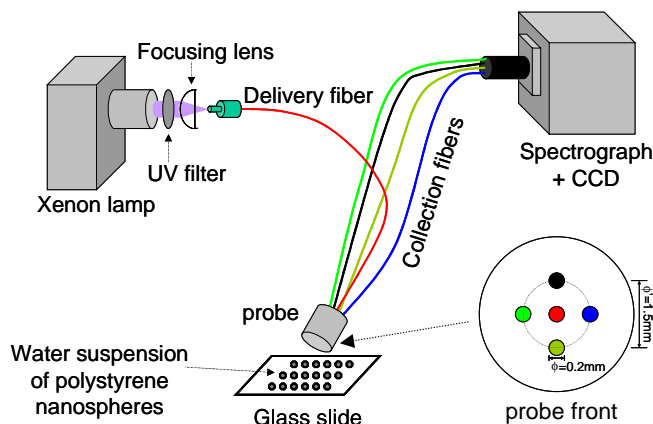


Fig. 1. The experimental setup of the UV LSS system and the design of the optical fiber probe.

illumination light. The broadband UV-VIS-infrared emission of the lamp was filtered by a UV filter (Edmund Industrial Optics) to remove the visible and infrared components. The remaining UV component was focused onto the distal end of the delivery fiber by a fused silica focusing lens (focal length = 38.0 mm). The collected light was transmitted to a spectrograph (InSpectrum-150, Acton Research Co.) coupled to a back-illuminated CCD (INS-150-250B, Hamamatsu) by means of fiber input. The light scattering spectrum was then recorded and analyzed.

The illumination spot on the sample was ~ 5 mm in diameter, and the distance between the spot and the proximal end of the delivery fiber was 6.6 mm. In order to avoid collecting the specular reflection from the sample surface, the probe was tilted at 30° angle to the normal of the sample surface. As determined by the probe geometry and the alignment, the collection angle is from 5.6° to 7.4° in the backward direction. The data acquisition times for the 33, 41, 63, and 81 nm sphere monolayers were 60, 60, 30, and 20 s, respectively. The acquisition times for 63 and 81 nm spheres were shorter because their signal levels were higher.

The experimental system was calibrated in order to correct for factors that introduce non-uniform spectral response, including the emission spectrum of the lamp, the profile of the UV filter, the transmission of the optical fibers, and the CCD quantum efficiency. The calibration was carried

out with a white standard (Ocean Optics, Inc.), which is a highly reflecting Lambertian reflector and reflects any incident UV-VIS-IR light uniformly into all solid angles regardless of its incident angle. Most importantly, the spectral response of a white standard is nearly constant over a wide spectral range. Its reflectance is 0.99 from near infrared down to 350 nm and slightly drops to 0.96 from 350 nm down to 250 nm. The calibrated signal $I_{\text{exp}}^{\text{cal}}(\lambda)$ is given as

$$I_{\text{exp}}^{\text{cal}}(\lambda) = R_0(\lambda) \cdot \frac{C(\lambda)}{C_0(\lambda)}, \quad (1)$$

where $C(\lambda)$ and $C_0(\lambda)$ are the CCD counts per second from a sample and from the white standard, and $R_0(\lambda)$ is the known reflectance of the white standard. In this way, the factors that introduce spurious non-uniform spectral response, such as the light source profile and CCD quantum efficiency, were cancelled out.

3. Experimental results and data analysis

In order to verify the significance of the UV LSS technique compared with conventional optical microscopy, we have observed the nanosphere samples and a sample of distilled water without nanospheres under an Olympus BX40 optical microscope. We have found that the microscopic images of the nanosphere samples are identical to that of the distilled water sample (photos not

shown), indicating optical microscopy can neither detect the existence nor differentiate the sizes of nanospheres. On the other hand, the backscattering spectra obtained from the nanospheres of different sizes are clearly distinct (Figs. 2–5), indicating that UV LSS is sensitive to nanoscale structures below the diffraction limit, which are beyond the detecting capability of conventional optical microscopy.

Several spectral features can be identified in our experimental data. In Fig. 2, the vertical axis represents the reflectance in the backward direction measured from all four samples. All spectral curves follow a power law, except for the wiggled patterns below 275 nm that are due to absorption peaks of polystyrene in this region. This power-law dependence is better illustrated by the nearly straight lines in Fig. 3, which is a log–log replot of the data in Fig. 2. We note that these lines are not parallel. Further investigation reveals that their slopes depend on the sizes of the scattering spheres (see below). However, the most significant differences among the spectral curves are their curvatures, as shown in Fig. 5, after rescaling the spectra between 275 and 390 nm to the same scale [0,1].

Our theoretical analysis is based on Mie theory, which is an exact solution of Maxwell equations on light scattering by a spherical scatterer of arbitrary size [17]. Mie solution requires only two parameters: the size parameter $x = \pi n_m d / \lambda$ and the relative refractive index $m = n_s / n_m$, where d , n_s , n_m and λ are the diameter of the scatterer, the

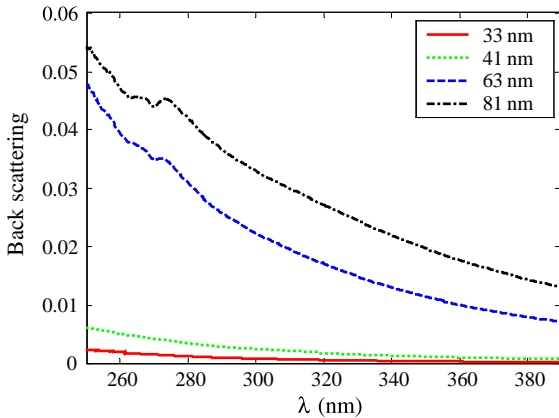


Fig. 2. The detected light scattering spectra of the nanospheres.

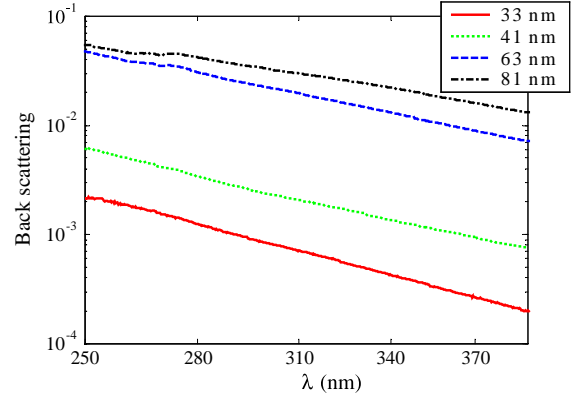


Fig. 3. The logarithmic replot of the light scattering spectra in Fig. 2. Note the horizontal axis is in fact in \log_{10} scale and the ticks are not equally spaced.

refractive indices of the scatterer and the medium, and the wavelength in vacuum, respectively. For accurate modeling, we have taken into account the dispersion of water (the medium) and polystyrene (the scatterer). In order to obtain the refractive index of water, we have applied the formulation from [18] at room temperature (27 °C) and ignored UV absorption by water. The refractive index of polystyrene is complex due to absorption, i.e.,

$$n_{\text{polystyrene}}(\lambda) = n_r(\lambda) - in_i(\lambda). \quad (2)$$

Here, the real part is given as [19]

$$n_r(\lambda) = A + B/\lambda^2 + C/\lambda^4, \quad (3)$$

where the constants A , B , and C are 1.5663 , 7.85×10^3 , and 3.34×10^8 , respectively, and λ is expressed in nanometers. The imaginary part of the refractive index is related to the absorption coefficient $\mu_a(\lambda)$ as

$$n_i(\lambda) = \frac{\lambda}{4\pi} \mu_a(\lambda). \quad (4)$$

There has been inconsistency in literature regarding the UV absorption of polystyrene [20–22]. Within our fitting range (275–390 nm), we have adopted the form

$$\mu_a(\lambda) = \begin{cases} \alpha \left[1 - \sqrt{(\lambda - \lambda_0)/(\lambda_1 - \lambda_0)} \right], & \text{for } \lambda_0 \leq \lambda \leq \lambda_1; \\ 0, & \lambda_1 < \lambda \end{cases} \quad (5)$$

as polystyrene absorption coefficient, where $\lambda_0 = 275$ nm and $\lambda_1 = 320$ nm. Its shape is similar

to the absorbance curve of polystyrene (in chloroform) reported in [22]. The choice of $\alpha = 5000 \text{ cm}^{-1}$ gives $n_i = 0.01$ at 275 nm.

Qualitatively, the power law dependence in Fig. 3 is expected by Rayleigh scattering. Rayleigh scattering states that the scattering cross-section of small particles is proportional to λ^{-4} , where λ is the wavelength. However, this is oversimplified for two reasons: the first, dispersion in the refractive index is not taken into account; and the second, the scatterer size d is ignored and the limit $d/\lambda \rightarrow 0$ is taken for granted. These conditions are not met in the general case of a small particle of finite size. Instead, one would expect

$$I_{\text{exp}}^{\text{cal}} \propto \lambda^{-\beta(d)}, \quad (6)$$

where exponent $\beta(d)$ is a function of the scatterer size. Further, the function form of $\beta(d)$ depends on the refractive index of the scatterer, which is uniquely determined by the scatterer's material. For example, polystyrene nanospheres and silica nanospheres will have different forms of $\beta(d)$. Quantitatively, Rayleigh scattering is inadequate and a more rigorous treatment is needed. We have used the exact Mie theory to calculate exponent $\beta(d)$ for light scattering of polystyrene nanospheres in water. In the meantime, we can also obtain the experimental β values from the slopes of the straight lines in Fig. 3. We identify the β -exponents for 33, 41, 63, and 81 nm spheres as 5.51 ± 0.03 , 4.61 ± 0.01 , 4.41 ± 0.02 , and 3.37 ± 0.01 , respectively. In Fig. 4, the solid curve is the Mie prediction on $\beta(d)$ after applying the wavelength dependent refractive indices of water [18] and polystyrene (Eqs. (2)–(5)), the dotted curve is the Mie prediction on $\beta(d)$ using constant refractive indices $n_{\text{water}} = 1.33$ and $n_{\text{polystyrene}} = 1.59$, while the four diamonds represent the experimental values. The wavelength range we used to determine β is 275–390 nm.

The first conclusion drawn from Fig. 4 is that the exponents significantly deviate from the value 4 of Rayleigh scattering, and $\beta = 4$ can *only* be attained at the limit $d/\lambda \rightarrow 0$ and when the refractive indices are constant. It can be further shown (not included in Fig. 4) that when the refractive indices are constant (either real or complex) with zero dispersion, the limit of β is always

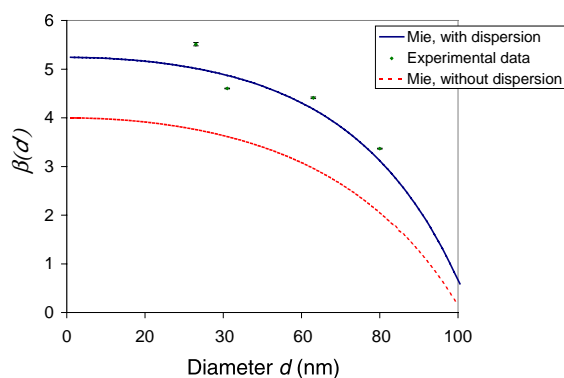


Fig. 4. The exponent β of the power law as predicted by Mie calculation (smooth curves) and given by measurements (diamond symbols). The solid curve is the prediction with dispersions in the refractive indices of water and polystyrene. The dotted curve is the prediction without dispersions: $n_{\text{water}} \equiv 1.33$, $n_{\text{polystyrene}} \equiv 1.59$.

4. The second conclusion is the monotonic dependence of β on sphere diameter d . This fact may provide a fast mapping scheme to find particle sizes from the β -exponent of their light scattering spectrum.

Rigorous data analysis requires a discrete inverse on experimental data. The theoretical prediction of light backscattered from a nanosphere of diameter d and at wavelength λ , $I_{\text{th}}(\lambda; d)$, is directly calculable from Mie theory. We further assume the size distribution of the nanospheres follows a Gaussian distribution, i.e.,

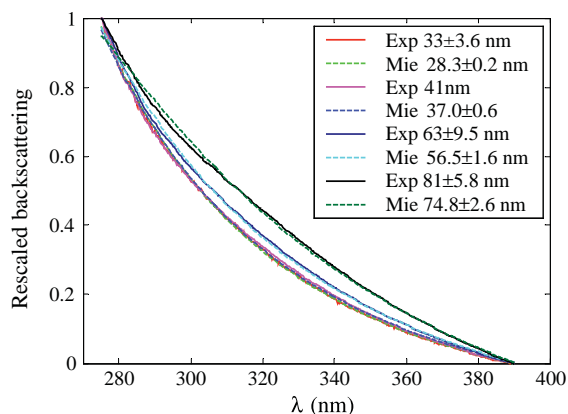


Fig. 5. The normalized spectra of backscatterings (solid curves) and their theoretical fit (dashed curves).

Table 1

The mean and standard deviation of the polystyrene nanospheres given by the manufacturer and our theoretical fit

Manufacturer values (nm)	d_0	33	41	63	81
	σ	3.6	Unspecified	9.5	5.8
Inverse results (nm)	d_0	28.3	37.0	56.5	74.8
	σ	0.2	0.6	1.6	2.6

$$\rho_{d_0,\sigma}(d) = \frac{1}{\sqrt{2\pi}\sigma^2} \exp\left[-\frac{(d-d_0)^2}{2\sigma^2}\right], \quad (7)$$

where d_0 and σ are the mean and the standard deviation of the nanosphere sizes. Then the theoretical prediction of the light backscattered from the sample is

$$I_{\text{th}}(\lambda; d_0, \sigma) = \int dx I_{\text{th}}(\lambda; x) \rho_{d_0,\sigma}(x). \quad (8)$$

Finally, the mean size d_0 and the standard deviation σ are determined as the minimal point of the objective function

$$\text{var}(d_0, \sigma) = \int d\lambda \left[a I_{\text{th}}(\lambda; d_0, \sigma) + b - I_{\text{exp}}^{\text{cal}}(\lambda) \right]^2. \quad (9)$$

In Eq. (9), the parameter a is introduced to model the overall factor between theoretical predictions and experimental data, and b is for background compensation. Table 1 lists the values provided by the manufacturer and the outcomes of our inverse procedure. The corresponding theoretical predictions of the light scattering spectra are also plotted in Fig. 5 (dashed curves) for comparison with experimental data (solid curves). As shown in Table 1, the values of nanoparticles' mean diameters obtained using UV LSS are in good agreement with those provided by the manufacturer: the inaccuracy of measurements is below ~ 6 nm for all types of nanoparticles, and the average relative error of measurements is $\sim 10\%$. Moreover, as can be seen in Fig. 5, the spectra predicted by Mie theory are in excellent agreement with the experimental data.

4. Conclusions

We have developed a UV LSS technique to detect nanoscale particles. By studying the back-

scattered light in the UV range, we are able to accurately determine the sizes of scattering spheres at nanoscale, even though optical microscopy fails to show the presence of these nanospheres. Nanometer resolution (~ 5 – 10 nm) has been achieved, which is more than an order of magnitude improvement over the results reported in recent literature [13] using angularly resolved forward light scattering, as well as the optical diffraction limit (~ 300 nm). Our technique can be potentially used in a variety of scientific and technological applications. For example, research in controlled-release drug delivery has shown [23] that reducing the particle size of poorly water-soluble drugs to nanometers can increase their bioavailability, and UV LSS can be used to monitor the nanoparticle size of the drugs during the pharmaceutical production. The high sensitivity and accuracy of UV LSS is useful in detecting and identifying viral particles, which have much simpler structures and chemical compositions than cells. However, further study of the optical properties of these biological entities is required for successful inverse of backscattering data. This is especially true for probing cell nanostructures, due to the complexity of cell environment. Nevertheless, UV LSS provides a new method and can complement the use of NSOM and AFM. Finally, the potential of UV LSS for non-biological applications, such as non-invasive monitoring of surface processes at nanoscale and monitoring of nanoparticle synthesis, is also significant.

Acknowledgements

This work was supported by the Institute for Bioengineering and Nanoscience in Advanced Medicine of Northwestern University.

References

- [1] C.J. Wang, M. Shim, P. Guyot-Sionnest, *Science* 291 (2001) 2390.
- [2] S. Sriraman, S. Agarwal, E.S. Aydil, D. Maroudas, *Nature* 418 (2002) 62.
- [3] J.Y. Maillard, *Rev. Med. Microbio.* 12 (2001) 63.
- [4] S. Bagley, M.W. Goldberg, J.M. Cronshaw, S.A. Rutherford, T.D. Allen, *J. Cell Sci.* 113 (2000) 3885.
- [5] S.A. Muller, A. Engel, *Micron* 32 (2001) 21.
- [6] F. de Lange, A. Cambi, R. Huijbens, B.D. Bakker, W. Rensen, M. Garcia-Parajo, N.V. Hulst, C.G. Figdor, *J. Cell Sci.* 114 (2001) 4153.
- [7] T. Enderle, T. Ha, D.F. Ogletree, D.S. Chemla, C. Magowan, S. Weiss, *Proc. Natl. Acad. Sci.* 94 (1997) 520.
- [8] T. Enderle, T. Ha, D.S. Chemla, S. Weiss, *Ultramicroscopy* 71 (1998) 303.
- [9] A. Engel, D.J. Muller, *Nature Struct. Biol.* 7 (2000) 715.
- [10] O.H. Willemsen, M.M. Snel, A. Cambi, J. Greve, B.G. De Grooth, C.G. Figdor, *Biophys. J.* 79 (2000) 3267.
- [11] A.T. Woolley, C. Guillemette, C.L. Cheung, D.E. Housman, C.M. Lieber, *Nature Biotechnol.* 18 (2000) 760.
- [12] J.H. Hafner, C.L. Cheung, A.T. Woolley, C.M. Lieber, *Prog. Biophys. Mol. Biol.* 77 (2001) 73.
- [13] M. Alexander, F.R. Hallett, *Appl. Opt.* 38 (1999) 4158.
- [14] L.T. Perelman, V. Backman, M. Wallace, G. Zonios, R. Manoharan, A. Nusrat, S. Shields, M. Seiler, C. Lima, T. Hamano, I. Itzkan, J. Van Dam, J.M. Crawford, M.S. Feld, *Phys. Rev. Lett.* 80 (1998) 627.
- [15] V. Backman, L.T. Perelman, J.T. Arendt, R. Gurjar, M.G. Muller, Q. Zhang, G. Zonios, E. Kline, T. McGillican, T. Valdez, J. Van Dam, M. Wallace, K. Badizadegan, J.M. Crawford, M. Fitzmaurice, S. Kabani, H.S. Levin, M. Seiler, R.R. Dasari, I. Itzkan, M.S. Feld, *Nature* 406 (2000) 35.
- [16] R. Gurjar, V. Backman, K. Badizadegan, R.R. Dasari, I. Itzkan, L.T. Perelman, M.S. Feld, *Nature Med.* 7 (2001) 1245.
- [17] H.C. van de Hulst, in: *Light Scattering by Small Particles*, John Wiley & Sons Inc., New York, 1957, Chapter 9.
- [18] A.H. Harvey, J.S. Gallagher, J.M.H.L. Sengers, *J. Phys. Chem. Ref. Data* 27 (1998) 761.
- [19] L.A. Matheson, J.L. Saunderson, in: R.H. Boundy, R.F. Boyer (Eds.), *Styrene, Its Polymers, Copolymers and Derivatives*, Reinhold Publishing Corp., New York, 1952, p. 517.
- [20] T. Inagaki, E.T. Arakawa, R.N. Hamm, M.W. Williams, *Phys. Rev. B* 15 (1977) 3243.
- [21] J.G. Carter, T.M. Jelinek, R.N. Hamm, R.D. Birkhoff, *J. Chem. Phys.* 44 (1966) 2266.
- [22] T. Li, C. Zhou, M. Jiang, *Polymer Bull.* 25 (1991) 211.
- [23] R.H. Muller, K. Peters, *Int. J. Pharm.* 160 (1998) 229.